Am J Physiol Cell Physiol 298: C702–C713, 2010.
First published December 16, 2009; doi:10.1152/ajpcell.00419.2009.

Regulation of vascular smooth muscle cell calcification by extracellular pyrophosphate homeostasis: synergistic modulation by cyclic AMP and hyperphosphatemia

Domenick A. Prosdocimo,[1] Steven C. Wyler,[1] Andrea M. Romani,[1] W. Charles O'Neill,[2] and George R. Dubyak[1]

[1]*Department of Physiology and Biophysics, School of Medicine, Case Western Reserve University, Cleveland, Ohio; and* [2]*Renal Division, Department of Medicine, Emory University School of Medicine, Atlanta, Georgia*

Submitted 16 September 2009; accepted in final form 14 December 2009

Prosdocimo DA, Wyler SC, Romani AM, O'Neill WC, Dubyak GR. Regulation of vascular smooth muscle cell calcification by extracellular pyrophosphate homeostasis: synergistic modulation by cyclic AMP and hyperphosphatemia. *Am J Physiol Cell Physiol* 298: C702–C713, 2010. First published December 16, 2009; doi:10.1152/ajpcell.00419.2009.—Vascular calcification is a multifaceted process involving gain of calcification inducers and loss of calcification inhibitors. One such inhibitor is inorganic pyrophosphate (PP_i), and regulated generation and homeostasis of extracellular PP_i is a critical determinant of soft-tissue mineralization. We recently described an autocrine mechanism of extracellular PP_i generation in cultured rat aortic vascular smooth muscle cells (VSMC) that involves both ATP release coupled to the ectophosphodiesterase/pyrophosphatase ENPP1 and efflux of intracellular PP_i mediated or regulated by the plasma membrane protein ANK. We now report that increased cAMP signaling and elevated extracellular inorganic phosphate (P_i) act synergistically to induce calcification of these VSMC that is correlated with progressive reduction in ability to accumulate extracellular PP_i. Attenuated PP_i accumulation was mediated in part by cAMP-dependent decrease in ANK expression coordinated with cAMP-dependent increase in expression of TNAP, the tissue nonselective alkaline phosphatase that degrades PP_i. Stimulation of cAMP signaling did not alter ATP release or ENPP1 expression, and the cAMP-induced changes in ANK and TNAP expression were not sufficient to induce calcification. Elevated extracellular P_i alone elicited only minor calcification and no significant changes in ANK, TNAP, or ENPP1. In contrast, combined with a cAMP stimulus, elevated P_i induced decreases in the ATP release pathway(s) that supports ENPP1 activity; this resulted in markedly reduced rates of PP_i accumulation that facilitated robust calcification. Calcified VSMC were characterized by maintained expression of multiple SMC differentiation marker proteins including smooth muscle (SM) α-actin, SM22α, and calponin. Notably, addition of exogenous ATP (or PP_i per se) rescued cAMP + phosphate-treated VSMC cultures from progression to the calcified state. These observations support a model in which extracellular PP_i generation mediated by both ANK- and ATP release-dependent mechanisms serves as a critical regulator of VSMC calcification.

ectonucleotide pyrophosphatase/phosphodiesterase-1; ANK; adenosine 3′,5′-cyclic monophosphate; ATP release

VASCULAR CALCIFICATION is associated with atherosclerosis, type 2 diabetes, end-stage renal disease, and aging (23, 43). It is characterized by increased vessel stiffness and loss of compliance that results in augmented arterial pulse wave velocity and pressure leading to left ventricular hypertrophy (9, 10, 46). Extracellular inorganic pyrophosphate (PP_i) is a critical inhibitor of calcification (50), and its importance is highlighted by the pathological condition of generalized arterial calcification of infants (GACI) caused by inactivating mutations in the ectonucleotide pyrophosphatase/phosphodiesterase-1 (ENPP1) gene. This gene encodes an extracellular PP_i-generating ecto-ATPase (39), and loss of ENPP1 function results in reduced PP_i accumulation and increased aortic calcification that can culminate in fatal aortic rupture (21, 39, 40).

Vascular calcification is characterized by the deposition of Ca^{2+} and inorganic phosphate (P_i) in the form of hydroxyapatite (HA) crystals within the medial or neointimal layers of blood vessels. This can involve induction of osteochondrogenic programs of gene expression in vascular smooth muscle cells (VSMC) (18). Recent studies have demonstrated the importance of extracellular P_i in acting not only as a substrate for HA formation but also an inducer of the gene expression programs that facilitate calcification (7, 8, 24). However, vascular calcification is a multifaceted process that involves not only the gain of inducers of calcification but also the loss of calcification suppressors, such as PP_i. Extracellular PP_i inhibits vascular calcification by directly disrupting the deposition of HA crystals. This action of PP_i requires its regulated accumulation and homeostasis in extracellular compartments. We recently described (38) an autocrine program of extracellular PP_i homeostasis in rat aortic VSMC that involves the coordinated functions of three known plasma membrane proteins and a molecularly undefined pathway of autocrine ATP release. The known PP_i-generating proteins include ENPP1, which catalyzes the hydrolysis of released ATP to produce PP_i, and progressive ankylosis disease susceptibility gene product ANK, an intrinsic plasma membrane protein that directly or indirectly mediates efflux of cytosolic PP_i. These parallel ATP release/ENPP1 and ANK pathways account for the accumulation of extracellular PP_i, and they are opposed by the alkaline phosphatase subtype tissue nonselective alkaline phosphatase (TNAP), an ectopyrosphosphatase that clears extracellular PP_i. On the basis of pharmacological experiments, we reported that ATP release/ENPP1 and ANK pathways each account for ~50% of the locally generated extracellular PP_i, with only a modest counteracting contribution from TNAP, in confluent monolayers of early-passage VSMC. This autocrine program allows these VSMC to condition their culture medium with micromolar concentrations of PP_i, which is sufficient for the steady-state suppression of matrix mineralization.

Address for reprint requests and other correspondence: G. R. Dubyak, Dept. of Physiology and Biophysics, Case Western Reserve Univ., School of Medicine, 2109 Adelbert Rd., Cleveland, OH 44106 (e-mail: george.dubyak@case.edu).

Hyperphosphatemia is a major predisposing factor for development of vascular calcification that most commonly occurs in the context of chronic kidney disease (14). However, progression of vascular calcification reflects the convergence of multiple genetic, metabolic, or endocrine perturbations, such as hyperphosphatemia, that separately elicit only minor or no increases in aberrant mineralization. This is highlighted in vivo in knockout mouse models that lack expression of either ENPP1 or ANK in which each genetic deficiency alone predisposes the animal to only mild and slowly developing calcification as a function of aging (21). The rate and severity of calcification are greatly potentiated when these animals are fed a high-phosphate diet. This same high-phosphate diet alone does not induce marked mineralization in wild-type animals. Studies with ex vivo aortic ring models have also indicated that elevated extracellular P_i alone is insufficient to induce mineralization (30). These organ-cultured aortic rings calcify in response to elevated P_i only when subjected to intentional mechanical injury or when supplemented with an excess of exogenous PP_i-degrading enzymes. In contrast to whole animal or ex vivo aortic ring models, in vitro cultures of VSMC can display marked calcification with elevated P_i as the only stimulus (33, 44). However, the efficacy and rate of the P_i-induced mineralization in VSMC cultures vary with species of origin, passage number, and clonal selection (24, 27, 28, 35, 48, 49, 52). Moreover, inclusion of cytokines and hormones such as parathyroid hormone, bone morphogenic proteins, VEGF, TNF-α, or vitamin D_3 can markedly potentiate this P_i-dependent calcification in vitro (5, 27, 32, 36, 49). These studies clearly demonstrate how various factors synergize with elevated extracellular P_i to induce modulation of VSMC phenotype and consequent calcification. It is equally important to consider the roles these procalcification signals may play in the expression and activity of PP_i homeostatic proteins in VSMC, particularly the PP_i-generating pathways involving ATP release/ENPP1 and ANK.

Demer and colleagues (15, 48, 49) have reported that activation of cAMP/protein kinase A (PKA) signaling markedly accelerates P_i-induced calcification in cultured bovine and murine VSMC models. Although this action of cAMP/PKA was correlated with altered accumulation of mRNAs encoding the TNAP, ENPP1, and ANK regulators of PP_i homeostasis, these studies did not include direct measurements of extracellular PP_i accumulation. Thus the mechanisms by which extracellular PP_i homeostasis may be dysregulated in this model of cAMP- and P_i-induced calcification remain unclear. We now report that these two procalcification stimuli act synergistically to suppress extracellular PP_i accumulation via reduced expression/activity of both ANK and the autocrine ATP release pathway that supports ENPP1-mediated PP_i production.

EXPERIMENTAL PROCEDURES

Materials. Sodium phosphate (Na_2HPO_4 and NaH_2PO_4) was from Fisher Scientific. Fetal bovine serum (FBS) and penicillin-streptomycin (P/S) were from Hyclone (Logan, UT). Low-glucose (1 g/l) Dulbecco's modified Eagle's medium (LG-DMEM), ATP standards (FL-AAS), TRIzol, adenosine-5′-triphosphate (ATP), cytidine-5′-triphosphate (CTP), adenosine (Ado), sodium pyrophosphate (PP_i), 3-isobutyl-1-methylxanthine (IBMX), 8-(4-chlorophenylthio)adenosine-3′,5′-cyclic monophosphate (CPT-cAMP), H-89, KT-5720, 8-(4-chlorophenylthio)-2′-*O*-methyl-cAMP (8-pCPT-2′-*O*-Me-cAMP), 9-dideoxyforskolin (dd-FSK), smooth muscle α-actin antibody (clone 1A4), firefly luciferase assay mix (FLAAM), adenosine-5′-phosphosulfate (APS), ATP-sulfurylase, β,γ-methylene ATP (MeATP), levamisole, cetylpyridinium chloride (CPC), *para*-nitrophenylphosphate (pNPP), and digitonin were from Sigma-Aldrich (St. Louis, MO). Forskolin (FSK) was from Alexis Biochemicals (San Diego, CA). Transgelin/SM22α (H-75), calponin 1 (Calp), PC-1 (L-20) (NPP1), and β-actin (C-11) antibodies were obtained from Santa Cruz Biotechnology (Santa Cruz, CA). GAPDH antibody was from Abcam (Cambridge, MA). Alizarin Red S was from GFS Chemicals (Columbus, OH). The RNeasy Mini Kit was from Qiagen (Valencia, CA). The Transcriptor first-strand cDNA synthesis kit was from Roche (Indianapolis, IN). Power SYBR Green PCR Master Mix was from Applied Biosystems (Foster City, CA). Predesigned quantitative PCR (qPCR) primer sets for rat β-actin (catalog no. PPR06570B), ENPP1 (PPR42431A), ANK (PPR52247A), TNAP (PPR52402A), and Runx2 (PPR53039A) were purchased from SA Biosciences (Frederick, MD), while qPCR primer pairs for rat GAPDH were designed with Primer3 software (http://frodo.wi.mit.edu) and synthesized by Operon Biotechnologies (Huntsville, AL).

VSMC isolation and cell culture. Primary rat aortic VSMC were isolated with an explant culture aortic ring model as previously described (4, 38). Male Sprague-Dawley rats (250 g) were euthanized by intraperitoneal injection of a saturated pentobarbital sodium solution (40 mg/kg body wt) as approved by the Case Western Reserve University Institutional Animal Care and Use Committee. The thoracic aorta was isolated under sterile airflow, and the adventitial and endothelial layers were gently removed to expose the media layer. The stripped media segment was sectioned into 2- to 3-mm rings that were placed onto a prescratched surface of a six-well plate incubated with 2 ml of LG-DMEM + 10% FBS, 1% P/S containing 0.9 mM P_i and 1.8 mM Ca^{2+}. The rings were maintained at 37°C in a 10% CO_2 humid atmosphere for 1 wk, after which primary VSMC were passaged weekly by trypsinization. All experiments utilized confluent monolayers of *passage 2–4* VSMC at ≥7 days after plating on six-well culture plates at a cell density of $0.1–0.4 \times 10^6$ cells/well. The cells were maintained in 2 ml of LG-DMEM + 10% FBS, 1% P/S with addition of fresh medium every 3–4 days.

Induction of calcification. In vitro VSMC calcification was induced by elevation of extracellular phosphate and/or FSK-mediated activation of cAMP signaling as previously described (15). VSMC were seeded at 0.1×10^6 cells/well and allowed to attach and grow for 2 days. The FBS-containing DMEM growth medium was then variously supplemented with *1*) 2.1 or 4.1 mM Na_2HPO_4/NaH_2PO_4 pH 7.4 to yield a final 3 or 5 mM phosphate concentration, respectively; *2*) 1 μM FSK; or *3*) a combination of 3 or 5 mM final phosphate plus 1 μM FSK. Parallel control wells were maintained in the standard FBS-containing DMEM growth medium. Media with the various supplements (elevated phosphate and/or forskolin) were replaced at 3-day intervals for up to 12 days. Parallel wells of similarly treated VSMC at the indicated days after induction with the various calcification stimuli were used for analysis of calcification, extracellular PP_i, and ATP homeostasis or altered gene expression, as described below.

Alizarin Red S-based measurement of calcification. Calcification was quantified by Alizarin Red S staining and organic extraction (11, 20, 47). VSMC monolayers were washed three times with 150 mM NaCl and fixed with 70% ethanol for 30 min at room temperature. The fixed cells were then washed three times with 25% ethanol followed by H_2O. After addition of Alizarin Red S (0.5%) pH 5.0 (1 ml/well), the cells were incubated for 10 min at room temperature before aspiration of the Alizarin Red solution. The wells were then washed four times with 1× PBS (pH 7.4) to remove unbound Alizarin Red, and the deposited Alizarin-Ca^{2+} complexes were extracted by the addition of 1–2 ml of 10% CPC. This extract was diluted 1:10 before measurement of the absorbance at 570 nm (A_{570}) with a Beckman DU640B spectrophotometer. The A_{570} values were normalized to total cellular protein, which was determined by the Bradford assay.

qPCR analysis of mRNAs encoding pyrophosphate homeostatic proteins. Total RNA from control or treated VSMC was isolated with TRIzol as previously described (38). RNA was purified and concentrated with the RNeasy Mini Kit (Qiagen). The purified RNA was primed with oligo(dT) primer, and first-strand cDNA was synthesized with the Transcriptor first-strand cDNA synthesis kit (Roche); qPCR analysis of ENPP1, TNAP, ANK, Runx2, and GAPDH transcript levels was performed with the StepOne-Plus Real-Time PCR system (Applied Biosystems). qPCR reactions were performed in 25-μl reaction volumes containing 1× Power SYBR Green PCR Master Mix, 400 nM primer mix, and 1:100 dilution of RT reaction product. Running conditions were 95°C for 10 min, followed by 40 cycles of 95°C for 15 s and 60°C for 60 s. Melting curves were performed at the end of each experiment, with all products demonstrating one predominant peak. Relative expression was calculated by the $\Delta\Delta C_t$ method (where C_t is threshold cycle) with the use of StepOne software v.2.1 and values normalized to GAPDH.

Quantitation of ATP and PP_i levels in extracellular medium samples. VSMC monolayers cultured under control or procalcification conditions were processed for analysis of extracellular ATP and PP_i accumulation as previously described (38). After removal of the growth or calcification medium, the intact cell monolayers were washed twice with PBS (pH 7.4) and then bathed in 1.2 ml of fresh basal salt solution (BSS) containing (in mM) 130 NaCl, 5 KCl, 1.5 $CaCl_2$, 1 $MgCl_2$, 25 Na-HEPES (adjusted to pH 7.5 at room temperature), and 5 mM glucose, with 0.1% BSA, to initiate test incubations at 37°C in the absence or presence of the indicated pharmacological agents. Extracellular aliquots of 100 μl were removed at various times (routinely 5, 60, and 120 min) after addition of BSS and analyzed for ATP and PP_i content. ATP and PP_i contents in the conditioned medium samples were quantified with a luciferase-based coupled enzyme assay (38). Heat-inactivated extracellular medium samples (75 μl) were mixed with 0.5 μl of 20 mM APS and 4 μl of concentrated FLAAM, and the resulting bioluminescence was recorded with a TD 20/20 luminometer as an indicator of ATP concentration. After this initial ATP-dependent bioluminescence, ATP-sulfurylase (0.01 U in 1 μl) was added to drive conversion of PP_i to ATP and bioluminescence was continuously recorded until a steady state was reached. This value was subtracted from the initial ATP-dependent bioluminescence value to give PP_i-dependent bioluminescence. Calibration curves with standard amounts of ATP and PP_i (1 nM to 1 μM) were generated for each experiment in the absence or presence of pharmacological inhibitors where relevant to assess possible effects of these inhibitors on the enzyme-linked reactions.

For some experiments, adherent VSMC monolayers were pulsed with 500 nM exogenous ATP after addition of BSS and extracellular samples (100 μl) were taken at specified time points and assayed for ATP and PP_i. Total cellular ATP content was determined by permeabilizing the VSMC monolayers with digitonin (50 μg/ml, 10 min, 37°C) and measuring the ATP released into the bathing medium.

High-performance liquid chromatography-based measurement of ENPP1 enzyme activity. ENPP1 enzyme activity in intact VSMC was assayed by measuring the metabolism of MeATP (38). VSMC monolayers were washed twice with 1 ml of PBS (pH 7.4) and then incubated in 1 ml of BSS supplemented with 300 μM MeATP. Samples of the extracellular BSS (100 μl) were taken at various times and heat inactivated (100°C) for 5 min. MeATP and its metabolites were chromatographically resolved with an Alltech C_{18} Adsorbosphere column that was isocratically eluted (1.3 ml/min) with 0.1 M KH_2PO_4 pH 6.0, 5% methanol. The eluted nucleotides were detected by absorbance at 254 nm. Chromatogram peak heights were determined with Data Ally v2.06 software, normalized to the initial MeATP concentration, and plotted versus time. Half-life ($t_{1/2}$) values were determined by a nonlinear regression one-phase exponential decay curve fit with GraphPad Prism v3.0 software.

Alkaline phosphatase activity. Alkaline phosphatase activity in whole cell lysates of VSMC was measured with 1 mM pNPP substrate as previously described (3, 31, 38).

Western blotting. Monolayers of adherent VSMC or HEK-293 cells stably transfected with human ENPP1 were extracted at 4°C with 200 μl/well RIPA buffer containing 0.5% Na-deoxycholate, 0.1% NP-40, and 0.1% SDS in 1× PBS pH 7.4 with freshly added protease inhibitors 100 μM PMSF, 2 μg/ml aprotinin, 500 μM DTT, and 2 μg/ml leupeptin and analyzed by SDS-PAGE, Western blotting, and chemiluminescence detection with horseradish peroxidase (HRP)-coupled secondary antibodies as previously described (13, 38). Primary antibodies were incubated overnight at 4°C in 6 ml of 4% nonfat milk with subsequent secondary antibody (2°Ab) incubations performed at room temperature for 1 h: SM-α actin (1/1,000; α-mouse 2°Ab 1/5,000), SM22α (1/300; α-rabbit 2°Ab 1/5,000), Calp (1/300; α-mouse 2°Ab 1/5,000), ENPP1 (1/250; α-goat 2°Ab 1/5,000), β-actin (1/500; α-goat 2°Ab 1/5,000), and GAPDH (1/1,000; α-mouse 2°Ab 1/7,500). Where indicated, the signal intensities of the HRP-labeled GAPDH bands were quantified by chemifluorescence imaging with a Typhoon Trio variable-mode imager (GE Healthcare Life Sciences). The human ENPP1 plasmid expression vector was provided by Dr. Robert Terkeltaub (University of California, San Diego).

Statistics. All experiments were repeated at least three times with different preparations of cultured VSMC. All data, unless otherwise stated, represent means ± SE, with statistical significance defined as $P < 0.05$ by two-tailed distribution with equal-variance Student's *t*-test.

RESULTS

Potentiation of P_i-induced VSMC matrix mineralization by cAMP signaling: time course and dependence on extracellular P_i concentration. We recently reported (38) that early-passage (*passages 2–4*) rat aortic VSMC cultures rapidly accumulate

extracellular PP_i via autocrine mechanisms that involve release of intracellular ATP and PP_i stores. We extended this culture model to the analysis of VSMC matrix mineralization in response to elevated extracellular P_i in the absence or presence of stimulated cAMP signaling. Only minor mineralization was observed in VSMC treated with either FSK (1 μM) alone or elevated P_i (3 or 5 mM) alone for up to 10 days (Fig. 1, *A* and *C*). Treatment with 3 or 5 mM P_i alone for 12 days increased mineral deposition, but not to statistically significant levels. In contrast, when coadministered, FSK + 5 mM P_i acted synergistically to increase the rate and magnitude of matrix calcification, which was significant within 9 days and maintained for up to 12 days (Fig. 1). FSK also potentiated matrix mineralization in VSMC challenged with 3 mM extracellular P_i, but this calcification required more prolonged cotreatment (Fig. 1*C*). For subsequent experiments, we routinely used VSMC cultures stimulated with 5 mM P_i + 1 μM FSK for 10 days as the model of induced matrix mineralization.

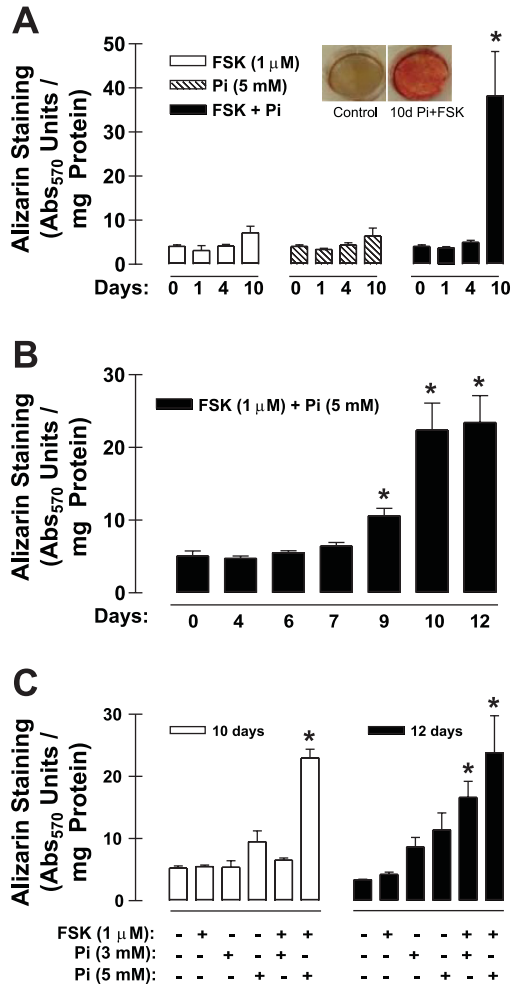

Fig. 1. Potentiation of inorganic phosphate (P_i)-induced vascular smooth muscle cell (VSMC) matrix mineralization by cAMP signaling: time course and dependence on extracellular P_i concentration. *A*: quantification of Alizarin Red S staining after treatment of VSMC for the indicated days in culture in the absence or presence of 1 μM forskolin (FSK), 5 mM P_i, or both 1 μM FSK + 5 mM P_i. Abs_{570}, absorbance at 570 nm. *Inset*: qualification of Alizarin Red S stain in VSMC treated for 10 days with the indicated stimuli. *B*: matrix mineralization time course of VSMC treated for the indicated days in culture in the absence or presence of 5 mM P_i + 1 μM FSK. *C*: P_i dose response (3 or 5 mM) in VSMC treated for 10 or 12 days in the absence or presence of 1 μM FSK. For all experiments, fresh growth medium supplemented with FSK, P_i, or FSK + P_i was added every 3 days. Data represent means ± SE; $n \geq 3$. *$P < 0.05$ vs. control.

VSMC matrix mineralization is correlated with decreased accumulation of extracellular PP_i and altered expression of PP_i homeostatic gene products. In vitro VSMC calcification is often characterized by the induction of osteochondrogenic markers and loss of VSMC differentiation proteins. However, the early-passage VSMC used in our experiments maintained high expression of the smooth muscle contractile marker proteins α-SM-actin, SM22α, and Calp regardless of their treatment protocol or calcification status (Fig. 2*A*). We observed a transient increase in mRNA (but not to statistically significant levels) encoding the osteoblast differentiation marker Runx2/Cbfa1 in response to elevated P_i alone or P_i + FSK, while FSK alone induced a progressive increase in Runx2 expression over 10 days (Fig. 2*B*). We also quantified TNAP, ANK, and ENPP1 mRNA levels in VSMC cultured under control or procalcification conditions (Fig. 2*B*). cAMP stimulation induced a progressive increase in TNAP expression in the absence or presence of elevated P_i. In contrast, the same cAMP stimulus caused a decrease in ANK expression that was maximal within 24 h in the absence of elevated P_i and further suppressed at 4 and 10 days in the presence of high P_i; elevated P_i alone did not significantly modulate ANK mRNA levels. A significant reduction in ENPP1 transcripts was observed only in VSMC stimulated with both FSK and high P_i for 10 days. These results suggest that multiple components of the extracellular PP_i homeostatic network are differentially regulated in response to cAMP stimulation alone or in combination with exposure to elevated P_i.

The alkaline phosphatase subtype TNAP is a calcification regulator that is necessary for normal physiological mineralization in bone (11). We confirmed previous reports (15) that FSK stimulation of VSMC causes a gradual and progressive increase in total alkaline phosphatase activity (which includes both TNAP and other alkaline phosphatase subtypes) in whole cell lysates (Fig. 2*C*). Notably, this cAMP-dependent elevation of alkaline phosphatase activity was modestly attenuated in VSMC additionally cultured with elevated P_i. Notably, elevated extracellular P_i alone did not increase TNAP transcripts or total alkaline phosphatase activity. These observations suggest that the robust mineralization phenotype observed at 10 days in VSMC costimulated with FSK and high P_i cannot be explained solely at the level of increased TNAP expression and alkaline phosphatase activity.

We measured the ability of VSMC to accumulate extracellular PP_i after FSK treatment in the absence or presence of elevated P_i. A twofold reduction in the rate of autocrine PP_i accumulation was observed in VSMC treated for 1 day with FSK (Fig. 2*D*). This reduction in extracellular PP_i accumulation rate was sustained when VSMC were continuously cultured in FSK-supplemented medium for up to 10 days (Fig. 2*D*; Fig. 3, *B* and *C*). Unexpectedly, VSMC exposed to high P_i (5 mM) alone for 24 h were characterized by a threefold increase in the rate of PP_i accumulation (Figs. 2*D* and 3*A*). However, this P_i-induced potentiation of PP_i accumulation was prevented when VSMC were additionally stimulated with FSK (Figs. 2*D* and 3*A*). The effect of hyperphosphatemia was transient; PP_i accumulation rates in VSMC cultured with elevated P_i for 4 (Fig. 2*D*) and 10 (Figs. 2*D* and 3*C*) days were

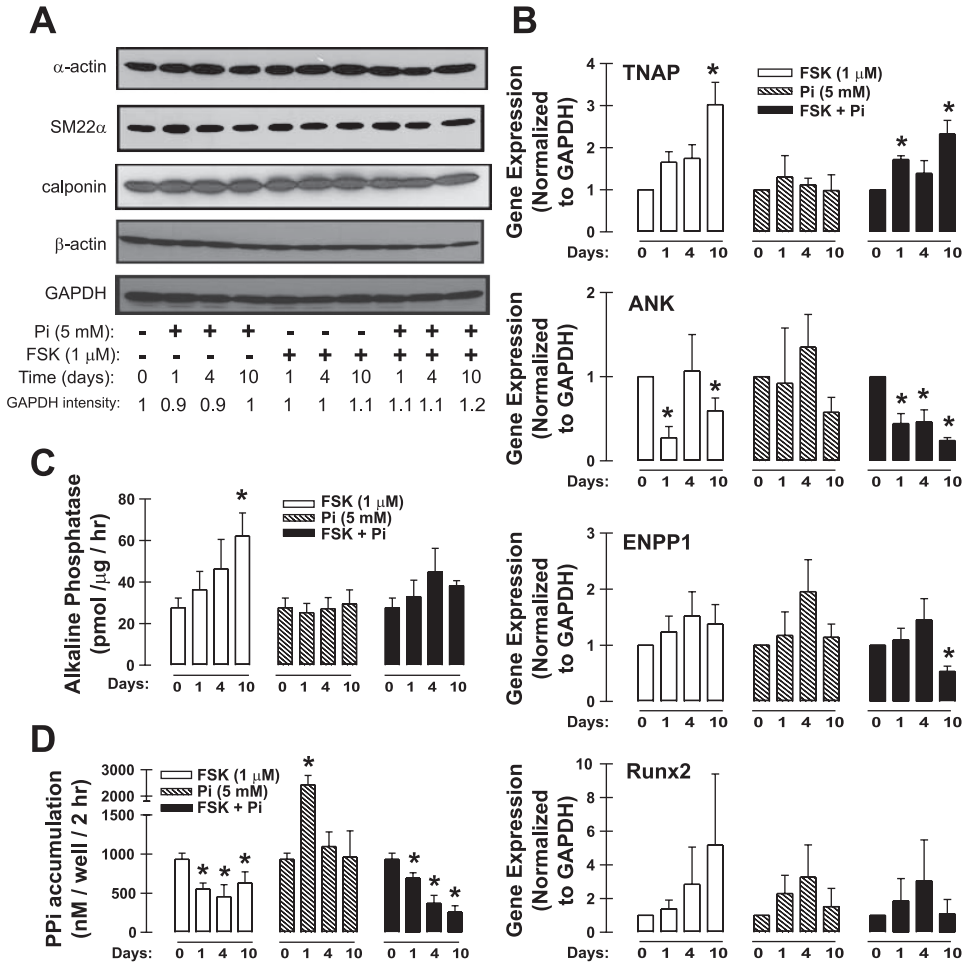

Fig. 2. VSMC matrix mineralization is correlated with decreased accumulation of extracellular inorganic pyrophosphate (PP_i) and altered expression of PP_i homeostatic gene products. *A*: Western blot of VSMC cell extracts probed for SMC marker proteins α-SM-actin, SM22α, and calponin for the indicated days in culture in the absence or presence of 1 μM FSK, 5 mM P_i, or FSK + P_i with β-actin and GAPDH as loading controls. Signal intensities of the GAPDH bands in each lane were quantified by chemifluorescence imaging and normalized relative to the GAPDH band intensity of control VSMC (1st lane). *B*: quantitative PCR (qPCR) analysis of PP_i homeostatic proteins tissue nonselective alkaline phosphatase (TNAP), ANK, and ectonucleotide pyrophosphatase/phosphodiesterase-1 (ENPP1), along with the osteochondrogenic marker Runx2 in VSMC treated for the indicated days in culture in the absence and presence of 1 μM FSK, 5 mM P_i, or FSK + P_i. *C*: alkaline phosphatase activity, measured by the rate of *para*-nitrophenylphosphate (pNPP) hydrolysis, in lysates of VSMC treated for the indicated days in culture in the absence or presence of 1 μM FSK, 5 mM P_i, or FSK + P_i. *D*: extracellular levels of PP_i generation at the 2 h time point after transfer of VSMC to basal saline assay medium that were treated for the indicated days in culture in the absence or presence of 1 μM FSK, 5 mM P_i, or FSK + P_i. Data represent means ± SE; $n \geq 3$. *$P < 0.05$ vs. control.

similar to those in control cells. Notably, VSMC costimulated for 10 days with FSK plus either 3 mM (Fig. 3*B*) or 5 mM (Figs. 2*D* and 3*C*) P_i were characterized by autocrine PP_i accumulation rates even lower than the reduced rate induced by FSK treatment alone. Together, these data indicate that the synergistic actions of cAMP and elevated phosphate on VSMC mineralization (Fig. 1) are well correlated with a markedly attenuated capacity for accumulation of extracellular PP_i.

Autocrine accumulation of extracellular PP_i is decreased in VSMC stimulated by cAMP: pharmacology, kinetics, and reversibility. The experiments in Fig. 2*D* and Fig. 3 indicated that the inhibitory effects of FSK on PP_i homeostasis were induced within 24 h and then steadily maintained over time. We further characterized the pharmacology and kinetics of this early response of VSMC to FSK. Cells pretreated with 1 μM FSK for 24 h were characterized by two- to threefold lower rates of extracellular PP_i accumulation relative to control cells (Fig. 4*A*). The PP_i accumulation rates in both control and FSK-treated VSMC were linear for ~2 h after transfer of the cells to PP_i-free assay medium (Fig. 4*A*). Notably, the reduced rate was observed even though the cells were washed and transferred to fresh FSK-free medium for the measurement of PP_i accumulation. This action of forskolin was time (Fig. 4*B*) and dose (Fig. 4*C*) dependent and required >12 h of treatment (Supplemental Fig. S1*A*).[1] Culturing VSMC with FSK for >12 h caused a sustained suppression of extracellular PP_i accumulation rate, but this effect was reversed on transfer of the cells back to FSK-free medium and tissue culture for an additional 24 h (Fig. 4*D*). These data indicate that the reduced capacity for extracellular PP_i accumulation by cAMP stimulation involves the regulation of gene expression, rather than posttranslational modification, of PP_i homeostatic proteins. The suppression of PP_i homeostasis by FSK reflected its specific action as a direct stimulator of cAMP accumulation because equimolar dd-FSK, an analog that does not activate adenylate cyclase, was without effect (Supplemental Fig. S1*B*). Moreover, similar decreases in PP_i accumulation rate were observed when cAMP signaling was stimulated with the phosphodiesterase inhibitor IBMX (200 μM) or the membrane-permeant cAMP analog CPT-cAMP (100 μM) (Fig. 4*E*). As noted in Fig. 2, the cAMP stimulus also modestly increased TNAP expression and alkaline phosphatase activity within 24 h. However, the reduced rate of extracellular PP_i accumulation observed in FSK-treated VSMC was not reversed by inclusion of 5 mM levamisole, a TNAP inhibitor, in the medium used to assay PP_i accumulation (Fig. 4*F*). This indicates that the increased alkaline phosphatase activity observed in Fig. 2*C* was not responsible for the

[1]The online version of this article contains supplemental material.

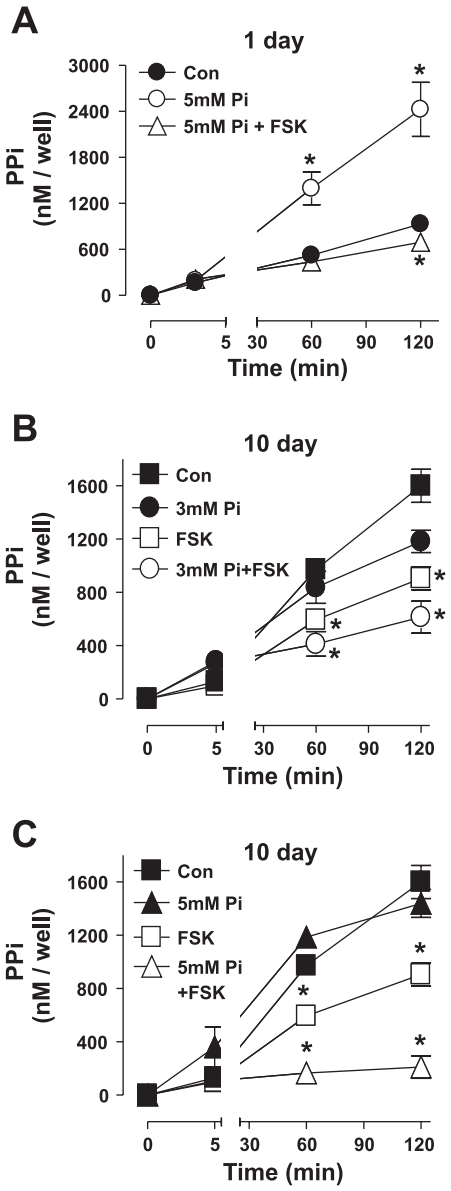

Fig. 3. cAMP signaling decreases the rate of extracellular PP_i accumulation by VSMC cultured with control or elevated levels of extracellular P_i. Time course of extracellular levels of PP_i generation following transfer of VSMC to basal saline assay medium that were treated for 1 day in the absence (Con) or presence of 5 mM P_i or 5 mM P_i + FSK (*A*); 10 days in the absence (Con) or presence of 3 mM P_i, 1 μM FSK, or 3 mM P_i + FSK (*B*); or 10 days in the absence (Con) or presence of 5 mM P_i, 1 μM FSK, or 5 mM P_i + FSK (*C*). Data represent means ± SE; $n \geq 3$. *$P < 0.05$ vs. control.

reduced rate of PP_i accumulation observed in VSMC treated with FSK for only 24 h.

We attempted to determine whether the inhibitory effects of cAMP on PP_i accumulation required PKA signaling pathways using H-89 and KT-5720, but neither of these PKA inhibitors reversed the effect of FSK (Supplemental Fig. S1*C*). Surprisingly, VSMC treated with H-89 or KT-5720 alone, in the absence of FSK, exhibited a greater than twofold reduction in extracellular PP_i generation similar to that induced by FSK alone. H-89 and KT-5720 can inhibit multiple kinases in addition to PKA (34). 8-pCPT-2′-*O*-Me-cAMP, a membrane-permeant cAMP analog that selectively activates the Epac cAMP-sensitive effector protein (but not PKA) (12), did not mimic the reduction in extracellular PP_i accumulation (Supplemental Fig. S1*D*) induced by the 8-pCPT-cAMP analog that activates both PKA and Epac signaling (Fig. 4*E*). Together, these data demonstrate that stimulation of cAMP signaling negatively regulates the ability of VSMC to generate extracellular PP_i.

ENPP1 ectonucleotidase activity is maintained at control levels in VSMC stimulated by cAMP or elevated extracellular P_i. Reduced levels of ENPP1 mRNA were observed only in VSMC cultured for 10 days with both FSK and high P_i (Fig. 2*B*). However, Western blot analysis indicated that total ENPP1 protein expression was reduced by FSK treatment in the absence or presence of elevated P_i at all time points, while a modest increase in ENPP1 protein was observed in cells stimulated with high P_i for 1 day, with levels decreasing below baseline at 4 and 10 days (Fig. 5*A*). To gauge the possible functional significance of these decreases in ENPP1 protein levels, we used an HPLC-based method to monitor the metabolism of extracellular MeATP, a specific substrate for ENPP family ecto-ATPases (38), by intact VSMC subjected to the various combinations and durations of cAMP or high phosphate stimuli (Fig. 5*B*). Figure 5*B*, *top*, illustrates the chromatograms of extracellular medium samples at 0, 10, 30, or 60 min after addition of 300 μM MeATP to control VSMC and indicates that these cells metabolize 50% of the nucleotide within 12 min to produce AMP, Ado, and (not pictured) inosine. No decreases in MeATP clearance rate (relative to control) were observed in any of the treated VSMC cultures (Fig. 5*B*, *inset*). Indeed, most of the treated cultures cleared MeATP at modestly faster rates (i.e., lower $t_{1/2}$ values). Thus the functional activity of ENPP1, as a cell surface ectonucleotidase, is maintained at control levels in FSK- and P_i-treated VSMC despite the reduction in ENPP1 protein in whole cell lysates.

To further characterize this dissociation between ENPP1 activity in intact cells and ENPP1 protein levels in cell lysates, we compared the abilities of control versus FSK-treated (1 day) VSMC to metabolize a pulse of 500 nM exogenous ATP and thereby produce extracellular PP_i in excess over that derived from endogenous sources (Fig. 5, *C* and *D*). Control VSMC rapidly metabolized the exogenous ATP (Fig. 5*E*) and increased extracellular PP_i by approximately twofold over that derived solely from autocrine metabolism (Fig. 5*C*). As noted above, FSK-treated VSMC were characterized by a twofold reduction in their ability to generate extracellular PP_i from endogenous stores (Fig. 5*D*). However, these cells hydrolyzed the 500 nM exogenous ATP at a control rate (Fig. 5*E*) to produce an additional 370 nM PP_i over that derived from the autocrine pathway (Fig. 5*D*). Thus reduced expression of ENPP1 as a functional cell surface nucleotidase does not play a major role in the attenuation of extracellular PP_i accumulation by VSMC stimulated by either increased cAMP signaling (Fig. 5, *B* and *D*) or elevated P_i (Fig. 5*B*).

Autocrine ATP release is decreased in VSMC costimulated by cAMP and elevated extracellular P_i. Although early and sustained decreases in both ANK expression and PP_i accumulation rate were induced by cAMP stimulation in the absence and presence of costimulation by high phosphate, VSMC subjected to both stimuli were characterized by even lower rates of autocrine PP_i generation (Fig. 2*D*). This suggested that the latter calcifying conditions induced modulation of additional pathways that generate extracellular PP_i. Increased

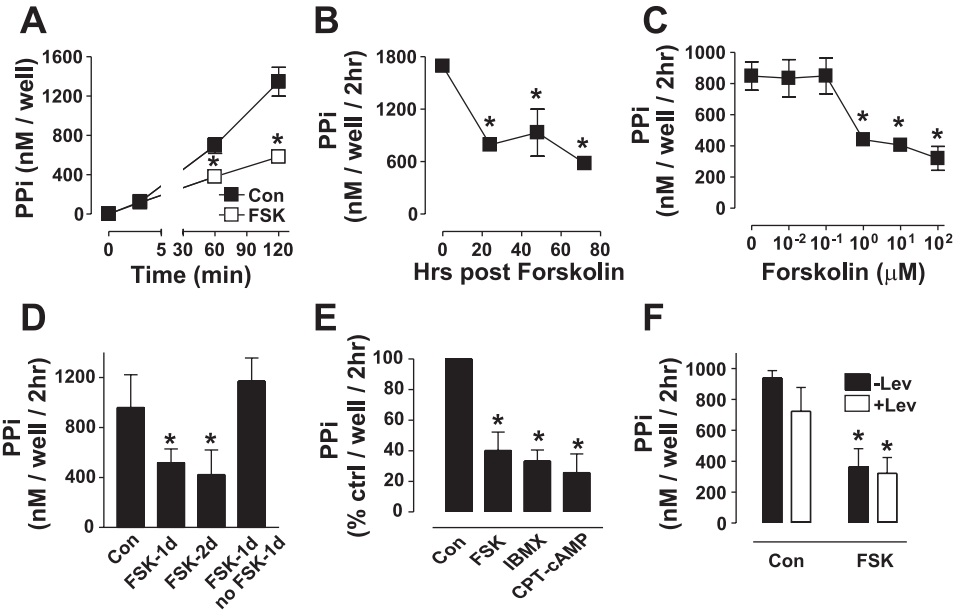

Fig. 4. cAMP-induced inhibition of autocrine PP_i accumulation in VSMC: pharmacology, kinetics, and reversibility. *A*: extracellular levels of PP_i generation after transfer of VSMC to basal saline assay medium that were treated for 24 h in the absence (Con) or presence of 1 μM FSK. *B*: time course of VSMC treated with 1 μM FSK; data represent the extracellular levels of PP_i generation at the 2 h time point after transfer of VSMC to basal saline assay medium. *C*: FSK dose response of VSMC treated for 24 h; data represent the extracellular levels of PP_i generation at the 2 h time point after transfer of VSMC to basal saline assay medium. *D*: extracellular levels of PP_i generation at the 2 h time point after transfer of VSMC to basal saline assay medium that were treated in the absence (Con) or presence of 1 μM FSK for 1 day (FSK-1d), 2 days (FSK-2d), or 1 day followed by the removal of FSK and incubated for an additional day (FSK-1d, no FSK-1d). *E*: extracellular levels of PP_i generation as % of control at the 2 h time point after transfer of VSMC to basal saline assay medium that were treated for 24 h in the absence (Con) or presence of 1 μM FSK, 200 μM 3-isobutyl-1-methylxanthine (IBMX), or 100 μM 8-(4-chlorophenylthio)adenosine-3′,5′-cyclic monophosphate (CPT-cAMP). *F*: extracellular levels of PP_i generation at the 2 h time point in the absence or presence of 5 mM levamisole (Lev) after transfer of VSMC to basal saline assay medium that were treated in the absence (Con) or presence of 1 μM FSK for 24 h. Data represent means ± SE; $n \geq 3$. *$P <$ 0.05 vs. control.

TNAP (Figs. 2*C* and 4*F*) and decreased ENPP1 (Fig. 5*B*) activity are unlikely mechanisms for this further reduction in PP_i accumulation rate. We therefore compared the abilities of the variously stimulated VSMC cultures to release ATP as the autocrine substrate for ENPP1-catalyzed production of extracellular PP_i. As we previously reported, autocrine ATP release from cultured VSMC is efficiently coupled to the ENPP1 ecto-ATPase such that only minor accumulation of ATP can be measured in the extracellular culture medium (38). Thus we utilized the ENPP1 competitive substrate MeATP (Fig. 5*B*) as a pharmacological tool to spare hydrolysis of endogenously released ATP and stabilize its extracellular accumulation. We observed a significant and progressive reduction in the ability of VSMC to release ATP when costimulated with FSK and elevated P_i for 4 and 10 days (Fig. 6). In contrast, ATP release was not significantly changed in cells treated with only FSK. VSMC exhibited a threefold increase in autocrine ATP release capacity when stimulated with high P_i alone for 1 day, followed by a return to control ATP release rates as the P_i stimulus was extended to 4 or 10 days. This latter pattern of ATP release was well correlated with the biphasic change in PP_i accumulation rates observed in VSMC stimulated with elevated extracellular P_i (Fig. 2*D*). Notably, no changes in total intracellular ATP content were observed in VSMC grown under any of the culture conditions (data not shown).

Matrix mineralization of VSMC costimulated by cAMP and elevated extracellular P_i is suppressed by exogenous ATP. The above experiments suggested that the ability of cAMP and high-phosphate costimulation to synergistically attenuate ATP release by VSMC reduces their capacity for extracellular PP_i generation and may thereby contribute to robust mineralization. To test this hypothesis, we compared extracellular Ca^{2+} deposition (by Alizarin Red S staining) in VSMC costimulated with FSK and elevated P_i for 10 days in the absence or presence of exogenously added PP_i, ATP, CTP, or Ado (each at 50 μM) (Fig. 7). As expected (37), exogenous PP_i completely suppressed the matrix mineralization induced by cAMP and high P_i costimulation. Notably, exogenous ATP similarly suppressed this mineralization phenotype. To assess the possible contribution of P_2 receptor signaling in ATP-induced rescue of VSMC from matrix mineralization, the VSMC cultures were alternatively supplemented with CTP, a nucleotide triphosphate that does not activate P_2 receptors but can serve as a substrate for ENPP1-mediated hydrolysis and PP_i generation. CTP mimicked the abilities of exogenous ATP or PP_i to suppress VSMC mineralization. Inhibition of mineralization by exogenous ATP could also reflect a contribution of Ado, a metabolite of extracellular ATP hydrolysis that signals through various G protein-coupled Ado receptors. However, exogenous Ado did not reverse the VSMC matrix mineralization induced by cAMP + high-P_i treatment.

DISCUSSION

This study describes novel mechanisms by which cAMP and elevated extracellular P_i act synergistically to induce VSMC calcification. Our experiments suggest that the synergy between these stimuli in driving matrix mineralization is medi-

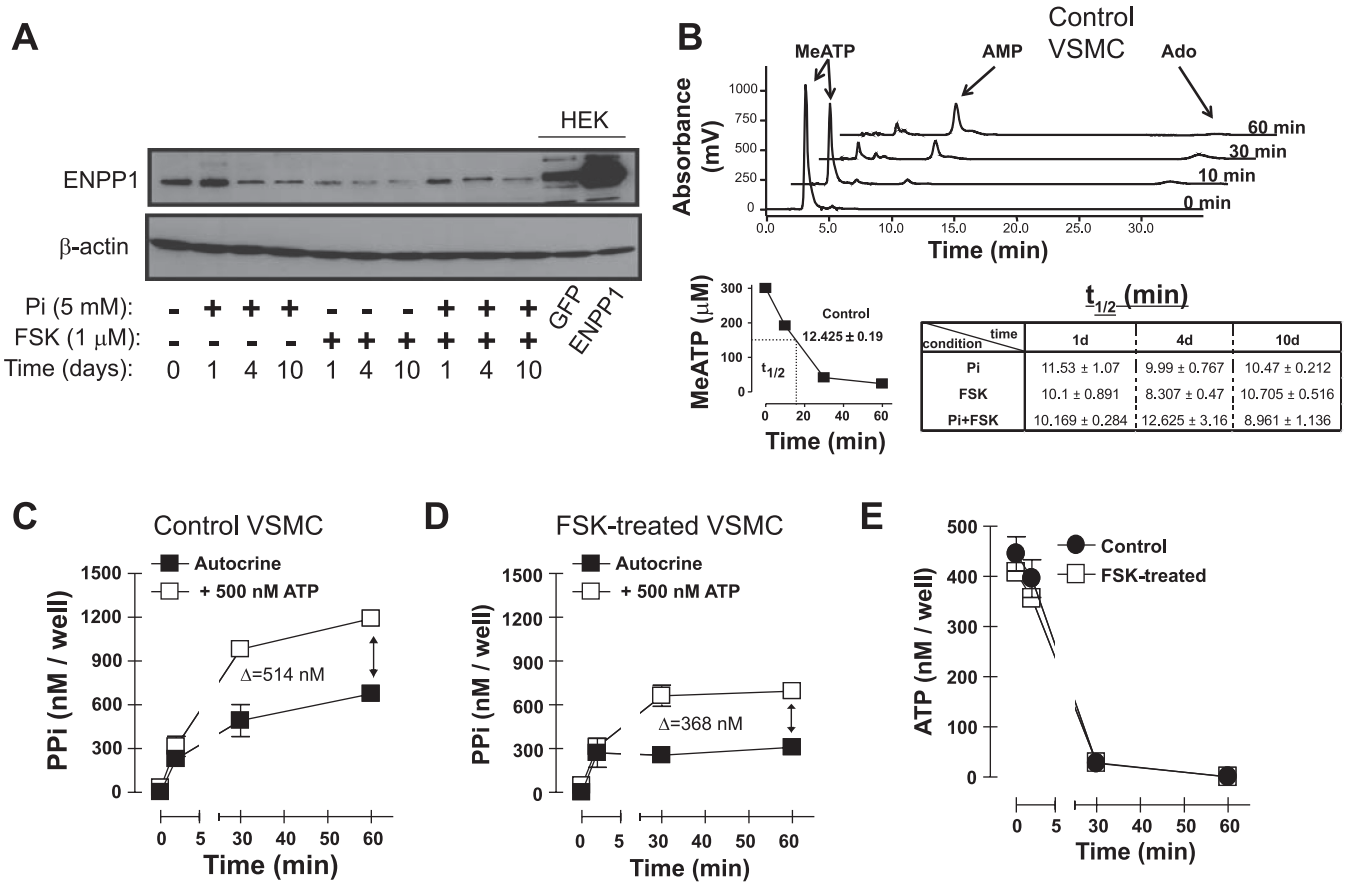

Fig. 5. ENPP1 ectonucleotidase activity is maintained at control levels in VSMC stimulated by cAMP or elevated extracellular P_i. *A*: ENPP1 Western blot of VSMC cell extracts treated for the indicated days in culture in the absence or presence of 1 μM FSK, 5 mM P_i, or FSK + P_i. HEK-293 cells stably expressing green fluorescent protein (GFP) or ENPP1 were used as controls (last 2 lanes on *right*). *B*: representative HPLC chromatogram of extracellular medium from intact control VSMC pulsed with 300 μM exogenous β,γ-methylene ATP (MeATP) and incubated for the indicated times. Ado, adenosine. *Inset*: cumulative time course data of MeATP (300 μM) hydrolysis in control VSMC based on calibrated peak heights detected by absorbance from the HPLC chromatograms; control half-life ($t_{1/2}$) = 12.425 ± 0.19 min. Table shows $t_{1/2}$ of 300 μM MeATP hydrolysis based on HPLC analysis of VSMC treated for the indicated days (d) in culture in the presence of 1 μM FSK, 5 mM P_i, or P_i + FSK. *C* and *D*: extracellular levels of PP_i after transfer of VSMC to basal saline assay medium incubated in the absence (autocrine) or presence of 500 nM ATP after treatment of VSMC for 24 h in the absence (*C*) or presence (*D*) of 1 μM FSK. *E*: extracellular levels of ATP after transfer to basal saline assay medium incubated in the presence of 500 nM ATP after treatment of VSMC in the absence (control) or presence of 1 μM FSK for 24 h. Data represent the range ± SD from a representative experiment repeated 3 times.

ated in part by suppression of two autocrine pathways for extracellular PP_i accumulation: *1*) the ANK-dependent efflux of cytosolic PP_i and *2*) a molecularly undefined ATP release pathway coupled to ENPP1-catalyzed ATP hydrolysis and PP_i generation. The decreased activities of these two mechanisms by which VSMC increase extracellular PP_i levels are coordinated with the increased activity of TNAP, a PP_i-degrading ectoenzyme and well-characterized inducer/marker of physiological calcification in bone and pathological mineralization in arteries. These observations support a model in which ANK- and ATP release-dependent mechanisms serve as critical regulators of extracellular PP_i generation and perturbation in their expression or function facilitates VSMC calcification. These findings also raise significant questions regarding the intracellular signaling pathways by which cAMP and elevated P_i act separately and convergently to regulate the expression and activity of the multiple gene products involved in extracellular PP_i homeostasis. It will also be important to determine whether modulation of these two pathways for PP_i accumulation does, or does not, occur in human VSMC and human disease states characterized by vascular calcification.

Our finding that stimulation of cAMP signaling for <24 h induced an ~50% decrease in the rate of extracellular PP_i accumulation was well correlated with a similar rapid decrease in ANK mRNA levels. In contrast, there were no significant changes in the expression or activity of the other major PP_i homeostatic proteins or functions—autocrine ATP release, ENPP1, or TNAP—during this early response to cAMP stimulation. Importantly, we previously reported (38) that a probenecid-sensitive mechanism provided ~50% of the extracellular PP_i-generating capacity of noncalcified VSMC. Together, our previous and new data suggest that reduced expression/trafficking of ANK to plasma membrane is the major mechanism underlying the rapid attenuation of extracellular PP_i generation in cAMP-stimulated VSMC. Unequivocal support for this conclusion will require quantification of ANK protein levels and localization in cultured VSMC. However, pilot studies with commercially available ANK antibodies failed to detect specific signals in whole cell lysates of these cells.

ANK is a 50-kDa plasma membrane protein with 8–12 predicted transmembrane domains that functions as either a direct PP_i transporter or a regulator of an as-yet unidentified

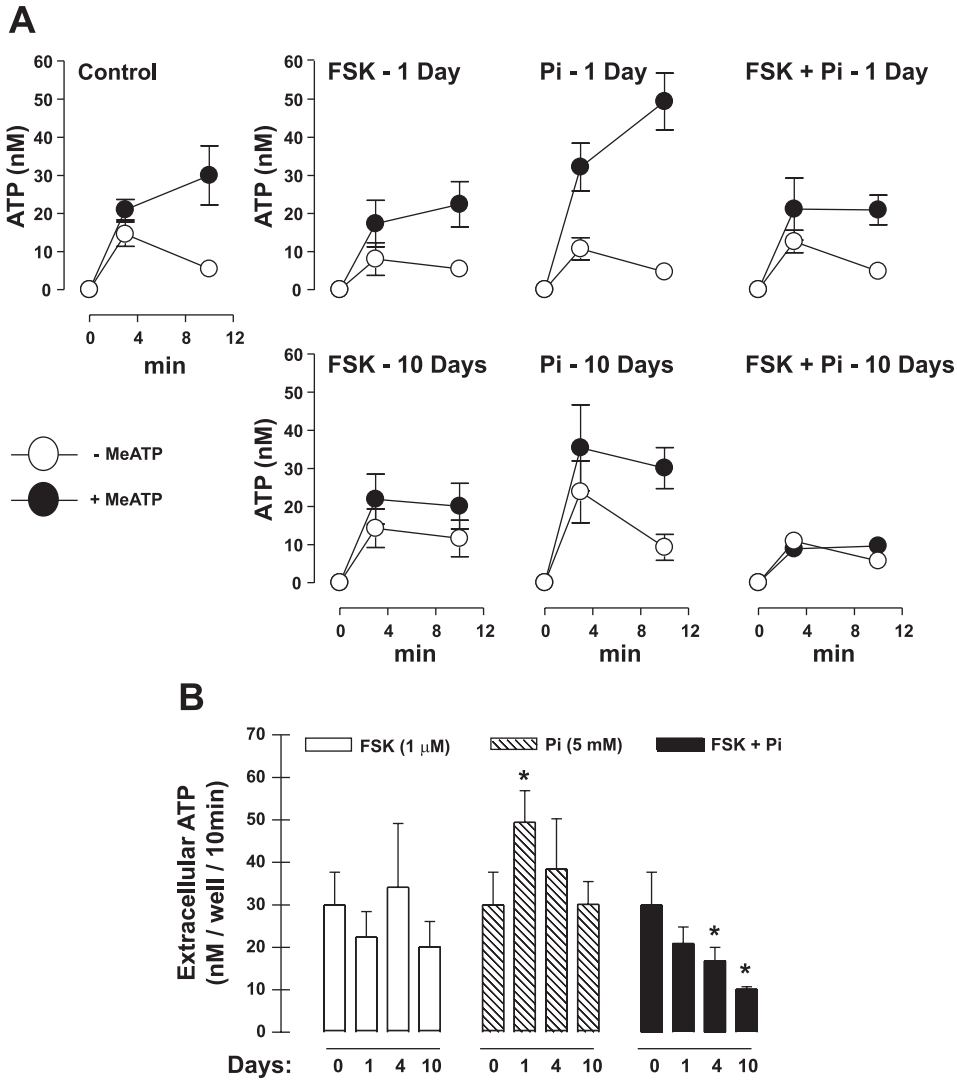

Fig. 6. Autocrine ATP release is decreased in VSMC costimulated by cAMP and elevated extracellular P_i. *A*: extracellular levels of ATP in the absence or presence of 300 μM MeATP in VSMC treated for 1 or 10 days in culture in the absence or presence of 1 μM FSK, 5 mM P_i, or FSK + P_i. *B*: cumulative data of extracellular ATP levels taken at the 10 min time point after transfer to basal saline assay medium in the presence of 300 μM MeATP of VSMC treated for the indicated days in culture in the absence or presence of FSK, P_i, or FSK + P_i. Data represent means ± SE; $n \geq 3$. *$P < 0.05$ vs. control.

PP_i transport protein (41, 53). The identification of ANK as a major target for rapid suppression by cAMP signaling is significant given previous findings that increased cAMP facilitates in vitro mineralization by osteoblasts and VSMC (15, 48, 49). However, these earlier studies emphasized the stimulatory effects of cAMP on induction/activity of proosteogenic transcription factors, such as Runx2/Cbfa-1 and osterix, which secondarily elicit—after several days—increased expression of effector proteins such as TNAP, matrix Gla protein (MGP), and osteospontin that directly modulate calcification. We also observed a gradual increase in TNAP mRNA (Fig. 2*B*) and enzyme activity (Fig. 2*C*) over 10 days of stimulation of VSMC by FSK. Analysis of Runx2 mRNA levels in the same extracts of FSK-stimulated VSMC showed a similar temporal trend of gradual (although not statistically significant) elevation (Fig. 2*B*). VSMC treated with elevated P_i + FSK (or P_i alone) exhibited a transient increase in Runx2 expression that returned to baseline levels before the robust matrix calcification. This transient increase is similar to the findings of Speer et al. (46), who recently reported that Runx2 expression within the in situ aortic VSMC of MGP-knockout mice is maximal at 2 wk before the massive vascular calcification that characterizes 4-wk-old MGP-null animals. Transient elevation of Runx2 is likely sufficient to increase the levels of osterix, a transcription factor that regulates expression of multiple gene products involved in matrix mineralization (23). In our VSMC model, ANK transcript levels were maximally decreased within 24 h after FSK treatment and this was temporally correlated with an at least twofold decrease in autocrine accumulation of extracellular PP_i that was insensitive to the TNAP inhibitor levamisole. Thus decreased expression of ANK and reduced PP_i generation precede increased expression of TNAP and Runx2 in cAMP-stimulated VSMC.

Another consequence of sustained cAMP stimulation on PP_i homeostasis was observed only when VSMC were costimulated by high extracellular P_i, and this involved a progressive decrease in autocrine ATP release. These changes in autocrine ATP release observed in cAMP- and P_i-treated VSMC likely reflect chronic modulation of the expression or activity of a molecularly undefined ATP release pathway (26). How this autocrine pool of ATP is exported from VSMC and how this export is attenuated by the combined phosphate and cAMP stimuli remain as key questions. Recent studies have focused on a variety of ATP-permeable channels or channel-like activ-

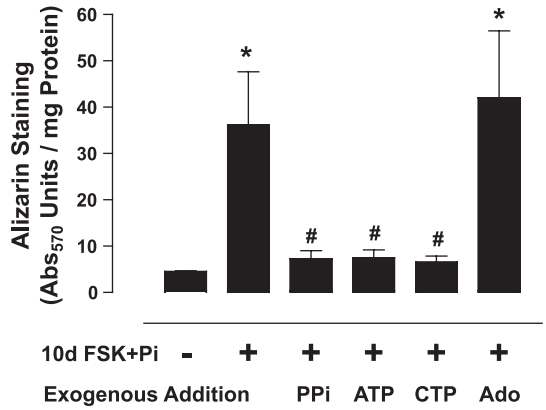

Fig. 7. Matrix mineralization of VSMC costimulated by cAMP and elevated extracellular P_i is suppressed by exogenous ATP. Quantification of Alizarin Red S staining after treatment of VSMC for 10 days in culture in the absence or presence of 1 μM FSK and 5 mM P_i and in the absence or presence of exogenous PP_i, ATP, CTP, or Ado (each at 50 μM). Fresh growth medium supplemented with FSK + P_i, exogenous PP_i, or nucleotides was added every 3 days. Data represent means ± SE; $n = 3$. $^*P < 0.05$ vs. control; $^{\#}P < 0.05$ vs. 10-day FSK + P_i.

ities as the major pathways for ATP export in multiple cell types (16, 17, 25, 26, 29, 42). Attenuated expression or activity of such channels likely underlies the decreased ATP release rate observed in calcifying VSMC. Regardless of the molecular basis for autocrine ATP release by VSMC, our experiments support the functional significance of this endogenous pool of ATP by showing that exogenous ATP can suppress the calcification of VSMC costimulated with cAMP and high P_i. A similar action of exogenous nucleotides in inhibiting mineralization has been described in primary rat osteoblasts (37).

Increases in extracellular P_i potentiate vascular calcification in two ways: *1*) by depositing within the extracellular matrix surrounding VSMC in the form of poorly soluble calcium phosphate crystals that include HA and other forms and *2*) by triggering intracellular signaling pathways as secondary response to enhanced influx via P_i transporters. HA crystal formation requires several days, and these crystals, when deposited adjacent to cells, have the potential to trigger additional modulation of cell function including inflammation, cellular damage, and apoptosis (6). However, high extracellular P_i can also elicit rapid changes in VSMC and other cell types that precede the obvious deposition of extracellular P_i-based crystals. Elevated extracellular P_i rapidly (within minutes to hours) stimulates MAP kinase and inhibits Akt kinase cascades in various cells (including VSMC), which, in turn, can induce transcriptional or posttranscriptional responses that impact cellular functions involved in the suppression or potentiation of mineralization (1, 2, 45). These latter responses to high extracellular P_i likely involve elevated influx of P_i via the type III Na-dependent P_i cotransporter Pit-1 to increase cytosolic P_i concentration (normally 0.5–1 mM) (28, 46). Our data indicate that elevated extracellular P_i also rapidly induces increased accumulation of extracellular PP_i in noncalcified VSMC via upregulation of an autocrine ATP release pathway. However, these increased rates of ATP release and PP_i accumulation were not sustained and returned to control values as the P_i stimulus was extended to 4 or 10 days.

Although there was a transient and modest increase in Runx2 expression in VSMC stimulated by high P_i alone (Fig. 2*B*), this was insufficient to induce a calcifying phenotype even after 10 days of sustained treatment. Other investigators have reported that elevated P_i alone can induce calcification in different VSMC models (33, 44). Notably, ex vivo organ cultures of freshly isolated aortic rings, which maintain VSMC in a physiological contractile phenotype, are remarkably resistant to high P_i-induced calcification in the absence of either deliberate mechanical damage or supplementation with exogenous alkaline phosphatase (30). Our VSMC cultures maintained high expression of multiple contractile marker proteins even when induced to calcify by costimulation with high phosphate and cAMP. Together, these observations in aortic rings and early-passage VSMC cultures suggest that contractile phenotype VSMC may support ectopic calcification reactions when subjected to stimuli that both suppress extracellular PP_i levels and induce cellular damage. It is also important to note that changes in expression of smooth muscle versus osteogenic marker genes in VSMC cultures during procalcification stimulation are often multiphasic because of changes in the relative fractions of VSMC at different phenotypic states. Previous studies in osteoblasts and chondrocytes have additionally indicated that changes in extracellular PP_i per se can modulate the expression of ANK, ENPP1, and TNAP via complex negative and positive feedback loops (10, 11, 19, 22). Thus the very early reduction in extracellular PP_i accumulation and ANK expression observed in FSK-treated VSMC may elicit feedback pathways that favor increased expression of ANK and ENPP1; the time course analyses of ANK and ENPP1 mRNA in Fig. 2*B* suggest such trends. Moreover, Huang et al. (15) observed that ANK and ENPP1 mRNA levels were increased in murine VSMC cultured for 7 days with 25 μM FSK + 5 mM glycerophosphate as an organic P_i donor.

It is noteworthy that extracellular PP_i homeostasis in VSMC and its perturbation by elevated phosphate involve the coordinated activities of at least three plasma membrane transport proteins, ANK, Pit-1, and the undefined ATP release channels, as well as two plasma membrane ectoenzymes, ENPP1 and TNAP. These proteins may be organized in functionally or structurally defined signaling complexes. Indeed, Wang et al. recently reported (51) that Pit-1 and ANK can be reciprocally coimmunoprecipitated from the plasma membrane extracts of chondrocytes, suggesting that the expression and function of these integral membrane proteins are linked. Given that decreased expression of ANK in cAMP-stimulated VSMC is correlated with suppression of the early high phosphate-induced increase in autocrine ATP release, it is tempting to speculate that ANK may also act as a direct or indirect positive regulator of ATP release channels.

ACKNOWLEDGMENTS

We thank Saneliso N. Masuku and Gregg DiNuoscio for technical assistance; Dr. Jeffery A. Beamish for calponin and SM22α antibodies; Dr. Cathy Carlin for GAPDH antibody; and Andrew E. Blum and Dr. Ozgur Ogut for useful discussions.

GRANTS

This work was supported in part by National Institutes of Health (NIH) Grants RO1-GM-36387 (G. R. Dubyak) and RO1-DK-69681 (W. C. O'Neill) and a grant from the Genzyme Renal Innovations Program (W. C. O'Neill). D. A. Prosdocimo was supported by NIH Grant T32-HL-07887.

DISCLOSURES

The authors are not aware of financial conflict(s) with the subject matter or materials discussed in this manuscript with any of the authors, or any of the authors' academic institutions or employers.

REFERENCES

1. **Beck GR Jr.** Inorganic phosphate as a signaling molecule in osteoblast differentiation. *J Cell Biochem* 90: 234–243, 2003.
2. **Beck GR Jr, Zerler B, Moran E.** Phosphate is a specific signal for induction of osteopontin gene expression. *Proc Natl Acad Sci USA* 97: 8352–8357, 2000.
3. **Brown NA, Stofko RE, Uhler MD.** Induction of alkaline phosphatase in mouse L cells by overexpression of the catalytic subunit of cAMP-dependent protein kinase. *J Biol Chem* 265: 13181–13189, 1990.
4. **Diglio CA, Grammas P, Giacomelli F, Wiener J.** Angiogenesis in rat aorta ring explant cultures. *Lab Invest* 60: 523–531, 1989.
5. **El-Abbadi MM, Pai AS, Leaf EM, Yang HY, Bartley BA, Quan KK, Ingalls CM, Liao HW, Giachelli CM.** Phosphate feeding induces arterial medial calcification in uremic mice: role of serum phosphorus, fibroblast growth factor-23, and osteopontin. *Kidney Int* 75: 1297–1307, 2009.
6. **Ewence AE, Bootman M, Roderick HL, Skepper JN, McCarthy G, Epple M, Neumann M, Shanahan CM, Proudfoot D.** Calcium phosphate crystals induce cell death in human vascular smooth muscle cells: a potential mechanism in atherosclerotic plaque destabilization. *Circ Res* 103: e28–e34, 2008.
7. **Giachelli CM.** The emerging role of phosphate in vascular calcification. *Kidney Int* 75: 890–897, 2009.
8. **Giachelli CM, Speer MY, Li X, Rajachar RM, Yang H.** Regulation of vascular calcification: roles of phosphate and osteopontin. *Circ Res* 96: 717–722, 2005.
9. **Guerin AP, Blacher J, Pannier B, Marchais SJ, Safar ME, London GM.** Impact of aortic stiffness attenuation on survival of patients in end-stage renal failure. *Circulation* 103: 987–992, 2001.
10. **Harmey D, Hessle L, Narisawa S, Johnson KA, Terkeltaub R, Millan JL.** Concerted regulation of inorganic pyrophosphate and osteopontin by akp2, enpp1, and ank: an integrated model of the pathogenesis of mineralization disorders. *Am J Pathol* 164: 1199–1209, 2004.
11. **Hessle L, Johnson KA, Anderson HC, Narisawa S, Sali A, Goding JW, Terkeltaub R, Millan JL.** Tissue-nonspecific alkaline phosphatase and plasma cell membrane glycoprotein-1 are central antagonistic regulators of bone mineralization. *Proc Natl Acad Sci USA* 99: 9445–9449, 2002.
12. **Holz GG, Chepurny OG, Schwede F.** Epac-selective cAMP analogs: new tools with which to evaluate the signal transduction properties of cAMP-regulated guanine nucleotide exchange factors. *Cell Signal* 20: 10–20, 2008.
13. **Hong S, Brass A, Seman M, Haag F, Koch-Nolte F, Dubyak GR.** Lipopolysaccharide, IFN-gamma, and IFN-beta induce expression of the thiol-sensitive ART2.1 Ecto-ADP-ribosyltransferase in murine macrophages. *J Immunol* 179: 6215–6227, 2007.
14. **Hruska KA, Mathew S, Lund R, Qiu P, Pratt R.** Hyperphosphatemia of chronic kidney disease. *Kidney Int* 74: 148–157, 2008.
15. **Huang MS, Sage AP, Lu J, Demer LL, Tintut Y.** Phosphate and pyrophosphate mediate PKA-induced vascular cell calcification. *Biochem Biophys Res Commun* 374: 553–558, 2008.
16. **Huang YJ, Maruyama Y, Dvoryanchikov G, Pereira E, Chaudhari N, Roper SD.** The role of pannexin 1 hemichannels in ATP release and cell-cell communication in mouse taste buds. *Proc Natl Acad Sci USA* 104: 6436–6441, 2007.
17. **Iovine MK, Gumpert AM, Falk MM, Mendelson TC.** Cx23, a connexin with only four extracellular-loop cysteines, forms functional gap junction channels and hemichannels. *FEBS Lett* 582: 165–170, 2008.
18. **Iyemere VP, Proudfoot D, Weissberg PL, Shanahan CM.** Vascular smooth muscle cell phenotypic plasticity and the regulation of vascular calcification. *J Intern Med* 260: 192–210, 2006.
19. **Johnson K, Goding J, Van Etten D, Sali A, Hu SI, Farley D, Krug H, Hessle L, Millan JL, Terkeltaub R.** Linked deficiencies in extracellular PP_i and osteopontin mediate pathologic calcification associated with defective PC-1 and ANK expression. *J Bone Miner Res* 18: 994–1004, 2003.
20. **Johnson K, Hashimoto S, Lotz M, Pritzker K, Goding J, Terkeltaub R.** Up-regulated expression of the phosphodiesterase nucleotide pyrophosphatase family member PC-1 is a marker and pathogenic factor for knee meniscal cartilage matrix calcification. *Arthritis Rheum* 44: 1071–1081, 2001.
21. **Johnson K, Polewski M, van Etten D, Terkeltaub R.** Chondrogenesis mediated by PPi depletion promotes spontaneous aortic calcification in NPP1−/− mice. *Arterioscler Thromb Vasc Biol* 25: 686–691, 2005.
22. **Johnson KA, Hessle L, Vaingankar S, Wennberg C, Mauro S, Narisawa S, Goding JW, Sano K, Millan JL, Terkeltaub R.** Osteoblast tissue-nonspecific alkaline phosphatase antagonizes and regulates PC-1. *Am J Physiol Regul Integr Comp Physiol* 279: R1365–R1377, 2000.
23. **Johnson RC, Leopold JA, Loscalzo J.** Vascular calcification: pathobiological mechanisms and clinical implications. *Circ Res* 99: 1044–1059, 2006.
24. **Jono S, McKee MD, Murry CE, Shioi A, Nishizawa Y, Mori K, Morii H, Giachelli CM.** Phosphate regulation of vascular smooth muscle cell calcification. *Circ Res* 87: E10–E17, 2000.
25. **Kreda SM, Seminario-Vidal L, Heusden C, Lazarowski ER.** Thrombin-promoted release of UDP-glucose from human astrocytoma cells. *Br J Pharmacol* 153: 1528–1537, 2008.
26. **Lazarowski ER, Boucher RC, Harden TK.** Mechanisms of release of nucleotides and integration of their action as P2X- and P2Y-receptor activating molecules. *Mol Pharmacol* 64: 785–795, 2003.
27. **Li X, Yang HY, Giachelli CM.** BMP-2 promotes phosphate uptake, phenotypic modulation, and calcification of human vascular smooth muscle cells. *Atherosclerosis* 199: 271–277, 2008.
28. **Li X, Yang HY, Giachelli CM.** Role of the sodium-dependent phosphate cotransporter, Pit-1, in vascular smooth muscle cell calcification. *Circ Res* 98: 905–912, 2006.
29. **Locovei S, Bao L, Dahl G.** Pannexin 1 in erythrocytes: function without a gap. *Proc Natl Acad Sci USA* 103: 7655–7659, 2006.
30. **Lomashvili KA, Cobbs S, Hennigar RA, Hardcastle KI, O'Neill WC.** Phosphate-induced vascular calcification: role of pyrophosphate and osteopontin. *J Am Soc Nephrol* 15: 1392–1401, 2004.
31. **Lomashvili KA, Garg P, Narisawa S, Millan JL, O'Neill WC.** Upregulation of alkaline phosphatase and pyrophosphate hydrolysis: potential mechanism for uremic vascular calcification. *Kidney Int* 73: 1024–1030, 2008.
32. **Mikhaylova L, Malmquist J, Nurminskaya M.** Regulation of in vitro vascular calcification by BMP4, VEGF and Wnt3a. *Calcif Tissue Int* 81: 372–381, 2007.
33. **Mune S, Shibata M, Hatamura I, Saji F, Okada T, Maeda Y, Sakaguchi T, Negi S, Shigematsu T.** Mechanism of phosphate-induced calcification in rat aortic tissue culture: possible involvement of Pit-1 and apoptosis. *Clin Exp Nephrol* 13: 571–577, 2009.
34. **Murray AJ.** Pharmacological PKA inhibition: all may not be what it seems. *Sci Signal* 1: re4, 2008.
35. **Nakano-Kurimoto R, Ikeda K, Uraoka M, Nakagawa Y, Yutaka K, Koide M, Takahashi T, Matoba S, Yamada H, Okigaki M, Matsubara H.** Replicative senescence of vascular smooth muscle cells enhances the calcification through initiating the osteoblastic transition. *Am J Physiol Heart Circ Physiol* 297: H1673–H1684, 2009.
36. **Neves KR, Graciolli FG, dos Reis LM, Graciolli RG, Neves CL, Magalhaes AO, Custodio MR, Batista DG, Jorgetti V, Moyses RM.** Vascular calcification: contribution of parathyroid hormone in renal failure. *Kidney Int* 71: 1262–1270, 2007.
37. **Orriss IR, Utting JC, Brandao-Burch A, Colston K, Grubb BR, Burnstock G, Arnett TR.** Extracellular nucleotides block bone mineralization in vitro: evidence for dual inhibitory mechanisms involving both P2Y2 receptors and pyrophosphate. *Endocrinology* 148: 4208–4216, 2007.
38. **Prosdocimo DA, Douglas DC, Romani AM, O'Neill WC, Dubyak GR.** Autocrine ATP release coupled to extracellular pyrophosphate accumulation in vascular smooth muscle cells. *Am J Physiol Cell Physiol* 296: C828–C839, 2009.
39. **Rutsch F, Ruf N, Vaingankar S, Toliat MR, Suk A, Hohne W, Schauer G, Lehmann M, Roscioli T, Schnabel D, Epplen JT, Knisely A, Superti-Furga A, McGill J, Filippone M, Sinaiko AR, Vallance H, Hinrichs B, Smith W, Ferre M, Terkeltaub R, Nurnberg P.** Mutations in ENPP1 are associated with "idiopathic" infantile arterial calcification. *Nat Genet* 34: 379–381, 2003.
40. **Rutsch F, Vaingankar S, Johnson K, Goldfine I, Maddux B, Schauerte P, Kalhoff H, Sano K, Boisvert WA, Superti-Furga A, Terkeltaub R.** PC-1 nucleoside triphosphate pyrophosphohydrolase deficiency in idiopathic infantile arterial calcification. *Am J Pathol* 158: 543–554, 2001.
41. **Ryan LM.** The ank gene story. *Arthritis Res* 3: 77–79, 2001.

42. **Schock SC, Leblanc D, Hakim AM, Thompson CS.** ATP release by way of connexin 36 hemichannels mediates ischemic tolerance in vitro. *Biochem Biophys Res Commun* 368: 138–144, 2008.
43. **Shao JS, Cai J, Towler DA.** Molecular mechanisms of vascular calcification: lessons learned from the aorta. *Arterioscler Thromb Vasc Biol* 26: 1423–1430, 2006.
44. **Shioi A, Nishizawa Y, Jono S, Koyama H, Hosoi M, Morii H.** Beta-glycerophosphate accelerates calcification in cultured bovine vascular smooth muscle cells. *Arterioscler Thromb Vasc Biol* 15: 2003–2009, 1995.
45. **Son BK, Kozaki K, Iijima K, Eto M, Nakano T, Akishita M, Ouchi Y.** Gas6/Axl-PI3K/Akt pathway plays a central role in the effect of statins on inorganic phosphate-induced calcification of vascular smooth muscle cells. *Eur J Pharmacol* 556: 1–8, 2007.
46. **Speer MY, Yang HY, Brabb T, Leaf E, Look A, Lin WL, Frutkin A, Dichek D, Giachelli CM.** Smooth muscle cells give rise to osteochondrogenic precursors and chondrocytes in calcifying arteries. *Circ Res* 104: 733–741, 2009.
47. **Thomas T, Gori F, Khosla S, Jensen MD, Burguera B, Riggs BL.** Leptin acts on human marrow stromal cells to enhance differentiation to osteoblasts and to inhibit differentiation to adipocytes. *Endocrinology* 140: 1630–1638, 1999.
48. **Tintut Y, Parhami F, Bostrom K, Jackson SM, Demer LL.** cAMP stimulates osteoblast-like differentiation of calcifying vascular cells. Potential signaling pathway for vascular calcification. *J Biol Chem* 273: 7547–7553, 1998.
49. **Tintut Y, Patel J, Parhami F, Demer LL.** Tumor necrosis factor-alpha promotes in vitro calcification of vascular cells via the cAMP pathway. *Circulation* 102: 2636–2642, 2000.
50. **Towler DA.** Inorganic pyrophosphate: a paracrine regulator of vascular calcification and smooth muscle phenotype. *Arterioscler Thromb Vasc Biol* 25: 651–654, 2005.
51. **Wang J, Tsui HW, Beier F, Tsui FW.** The CPPDD-associated ANKH M48T mutation interrupts the interaction of ANKH with the sodium/phosphate cotransporter PiT-1. *J Rheumatol* 36: 1265–1272, 2009.
52. **Watson KE, Bostrom K, Ravindranath R, Lam T, Norton B, Demer LL.** TGF-beta 1 and 25-hydroxycholesterol stimulate osteoblast-like vascular cells to calcify. *J Clin Invest* 93: 2106–2113, 1994.
53. **Zaka R, Williams CJ.** Role of the progressive ankylosis gene in cartilage mineralization. *Curr Opin Rheumatol* 18: 181–186, 2006.